

# 2

## **SURFACE MORPHOLOGY AND LATERAL DISTRIBUTION OF SELF- ASSEMBLED $\text{In}_{0.5}\text{Ga}_{0.5}\text{As}$ NANOSTRUCTURES GROWN ON GaAs (100) SUBSTRATES**

Didik Aryanto  
Zulkafli Othaman  
Abd. Khamim Ismail  
Shahrizar Roslan  
Rosnita Muhammad  
Imam Sumpono  
Amira Saryati Ameruddin

This paper investigates the size, density and uniformity of double layer  $\text{In}_{0.5}\text{Ga}_{0.5}\text{As}$  nanostructures as a function of GaAs buffer layer thickness. Observation of surface morphology by atomic force microscopy (AFM) and field emission scanning electron microscopy (FESEM) shows that the dots formation depends strongly on the GaAs buffer layer thickness. The size of dots reduce with the increase in the buffer layer thickness. Self-assembled  $\text{In}_{0.5}\text{Ga}_{0.5}\text{As}$  nanostructures grown on GaAs (100) substrate with a 200 nm thick GaAs buffer layer has high-dot density ( $4.68 \times 10^{10} \text{ cm}^{-2}$ ) and more uniform dot size. Increasing

and decreasing of the buffer layer thickness causes the density of small dots to be reduced with several large dots (nano-islands) distributed randomly on the surface. The GaAs buffer and spacer layer thickness in the growth of  $\text{In}_{0.5}\text{Ga}_{0.5}\text{As}$  nanostructures has important effect on the dots formation.

## 2.1 OVERVIEW

The self-assembled formation of quantum dot structures has been shown to follow in a Stranski-Krastanow (S-K) growth mode, in which the island formation occurs following the initial two-dimensional growth [1]. This growth mode has been shown to produce dots in the form of coherent nano-islands in a variety of strained hetero-combinations, for example Ge/Si [2, 3], InAs/GaAs [4,5,6], InAs/InP [7,8], and  $\text{In}_x\text{Ga}_{1-x}\text{As}/\text{GaAs}$  [9,10]. Self-assembled quantum dots using the Stranski–Krastanow growth mode has been shown to possess excellent optical properties reflecting their discrete density of states [10] and to realize various optoelectronic devices such as low-threshold, temperature insensitive laser diodes [11,12,13] and semiconductor optical amplifiers [12]. Most recently, the atom-like properties of their electronic state were exemplified by the generation of single-photon emitters [14].

Self assembled quantum dots formed by the Stranski-Krastanow transition of highly strained  $\text{In}_x\text{Ga}_{1-x}\text{As}$  grown on GaAs by MBE (molecular beam epitaxy) or MOVPE (metalorganic vapor phase epitaxy) have recently demonstrated by several groups [4, 5, 6, 10]. Recently, self-assembled  $\text{In}_x\text{Ga}_{1-x}\text{As}/\text{GaAs}$  quantum dots, based on their novel physical properties has shown potential application in optical and electronic devices such as quantum disc lasers [15], quantum dot lasers [11,12,13], solar cells [16], etc. This is due to the optimization of the  $\text{In}_x\text{Ga}_{1-x}\text{As}$  quantum dots growth which produces more uniform, homogeneous and high density of dots [10]. The control over the size, density, regularity

and integrity of quantum dots is essential for the realization of high performance quantum dot devices.

Self-assembled quantum dots can be formed and derived by strain in highly lattice-mismatched semiconductor materials via hetero-epitaxy [10]. Epitaxial growth in the layer stage of deposition can exert a strong influence on the surface morphology of the multilayer nanostructures. The evolution of surface morphology during epitaxial growth is the result of a delicate interplay between the deposition of atom onto the surface and the subsequent relaxation of the surface profile through surface diffusion and other kinetic process of the surface toward equilibrium [17]. Therefore, the structural and optical properties of self-assembled quantum dots are expected to be influenced by the surface disorientation.

Lattice mismatch between the epilayer and the substrate creates undesirable lattice defects, especially misfit dislocation and threading dislocation of the interface. Compositionally graded buffer layer is particularly efficient for reducing both the misfit dislocation density near the top of buffers and in the active parts of hetero-structure and the threading dislocation density [18]. However misfit dislocation and threading dislocation density is not the only parameter for evaluating the buffer layer quality; the surface roughness and the symmetry of the strain relaxation must be taken into account as well [19]. GaAs epilayer was grown on misoriented GaAs (001) substrate have typical pattern with clearly resolved slashes taken from a misoriented GaAs(001) surface. For small misoriented and less well-ordered steps arrays, however the clear diffraction features are diminishing [20]. Growth of In<sub>0.5</sub>Ga<sub>0.5</sub>As quantum dots has examined the wafer-to-wafer differences in quantum dot density as a function growth conditions.

Studies have shown that different growth condition can lead to quite different surface morphologies from step flow growth mounding [5,17,21]. It might be expected that these differences in buffer morphology would lead to differences in quantum dots formation. Influence of substrate preparation and buffer layer growth condition on buffer layer roughness was studied by Roskho

et al. [9]. Lai et al. [10] has studied  $\text{In}_{0.5}\text{Ga}_{0.5}\text{As}$  quantum dots grown with Gas Source-MBE system by sequential and migration enhanced epitaxial techniques. Many studies were conducted to investigate the effect of growth parameters toward uniformity, high density, optoelectronic and electronic properties of quantum dots.

Each study uses different buffer layer thickness, such as 840 nm [22], 500 nm [10, 23], 120 nm [24], and 100 nm [25]. GaAs buffer layer thickness was grown on GaAs (100) substrate before growth of  $\text{In}_x\text{Ga}_{1-x}\text{As}$  quantum dots. However, results of self-assembled quantum dots grown by other groups are different in terms of size, density and uniformity. In this paper we reported morphology and lateral distribution from  $\text{In}_{0.5}\text{Ga}_{0.5}\text{As}$  quantum dots with various buffer layer thicknesses. The  $\text{In}_{0.5}\text{Ga}_{0.5}\text{As}$  nanodots were grown using MOVPE in Stranski-Krastanow growth mode. The morphology and structural analysis were carried out by AFM and FESEM.

## **2.2 EXPERIMENTAL PROCEDURE**

Self-assembled  $\text{In}_{0.5}\text{Ga}_{0.5}\text{As}$  nanostructures were grown on semi-insulating GaAs (100) substrates using MOVPE technique in the Stranski-Krastanow mode. The MOVPE growth technique uses the group III metal alkyls and group V hydride. The group III source materials were trimethylgallium (TMGa) and trimethylindium (TMIn), held in temperature controlled baths at  $-3.5^\circ\text{C}$  and  $17^\circ\text{C}$ , respectively, while arsine diluted to 10% in hydrogen was the group V source. Palladium diffused hydrogen was used as the carrier gas. The temperature and pressure of the metal-organic precursors were fixed to control the vapor pressure in the bubbler.

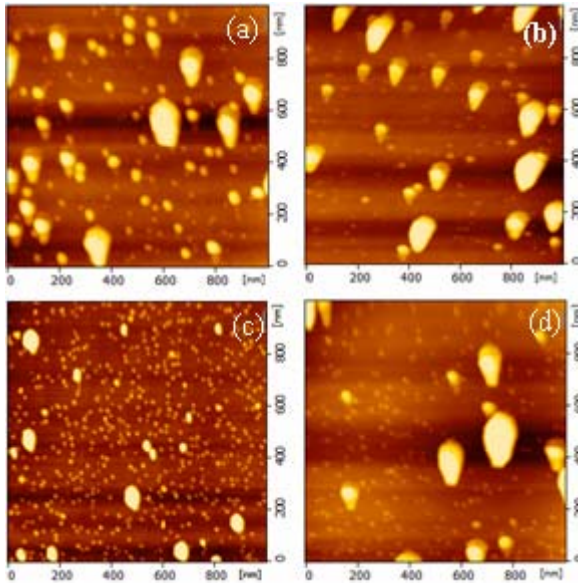


**Figure 2.1.** AFM images of double layer  $\text{In}_{0.5}\text{Ga}_{0.5}\text{As}$  nanostructures on GaAs (100) substrates with different buffer layer thickness (a) 100 nm; (b) 150 nm; (c) 200 nm and (d) 300 nm.

The  $\text{In}_{0.5}\text{Ga}_{0.5}\text{As}$  nanostructures and GaAs buffer layer were grown at pressure of 76 Torr. The native oxides on the substrates were thermally dissociated at 750 °C under As ambient in the III-V growth chamber. The thick GaAs buffer layer was grown at 650 °C with different thickness for each sample (100 nm, 150 nm, 200nm, and 300nm). All structures of GaAs buffer layer were grown with a V/III ratio fixed at 80 during deposition. Self-assembled  $\text{In}_{0.5}\text{Ga}_{0.5}\text{As}$  nanodots were grown at 550 °C. Before  $\text{In}_{0.5}\text{Ga}_{0.5}\text{As}$  nanostructures deposition, the reactor temperature was stabilized at the  $\text{In}_{0.5}\text{Ga}_{0.5}\text{As}$  nanostructures growth temperature (550 °C) under flow of  $\text{AsH}_3$  to protect the surface. The flow rate of TMGa, TMIIn and  $\text{AsH}_3$  were 2 sccm, 100 sccm, and 32 sccm, respectively, with a V/III ratio was fixed at 10 during the deposition of  $\text{In}_{0.5}\text{Ga}_{0.5}\text{As}$  nanostructures. Growth parameters and time were constant throughout the growth of  $\text{In}_{0.5}\text{Ga}_{0.5}\text{As}$  nanostructures. After deposition

In<sub>0.5</sub>Ga<sub>0.5</sub>As nanostructures, 25 nm GaAs spacer layer was grown at the same parameter as the GaAs buffer layer. Finally, self-assembled In<sub>0.5</sub>Ga<sub>0.5</sub>As nanostructures were deposited on the GaAs spacer layer. The morphology and surface density analysis of In<sub>0.5</sub>Ga<sub>0.5</sub>As nanostructures on the top layer were performed with AFM and FESEM.

### **2.3 RESULTS AND DISCUSSION**

Surface morphology of the In<sub>0.5</sub>Ga<sub>0.5</sub>As/GaAs nanostructures with different buffer layer thickness was characterized using AFM. Figure 2.1 shows the AFM images of In<sub>0.5</sub>Ga<sub>0.5</sub>As nanostructures with different buffer layer thicknesses (100 nm, 150 nm, 200 nm and 300 nm). The images show that the formation of the nanostructures was not uniform, with size variation and non-uniform distribution of nanostructures. In several areas of all samples, nanostructure of different shapes and sizes are clearly visible with small dots and some larger dots distributed randomly on the surface. The nucleation and coalescence process of smaller dots in forming larger dots were not fully completed.

The AFM images show that size, density and distribution of In<sub>0.5</sub>Ga<sub>0.5</sub>As nanostructures is different for different buffer layer thickness. It indicates that the growth of GaAs buffer layer prior to the self-assembled growth of In<sub>0.5</sub>Ga<sub>0.5</sub>As nanostructures is essential in improving the surface morphology of its epilayer. This transition from the layer growth to the island formation results from a complex process, which includes lattice strain and kinetic processes like surface diffusion and the incorporation of adatoms [26]. Atoms impinging on the surface of the substrate may be desorbed from the surface immediately or after undergoing some surface diffusion. In this Stranski-Krastanow growth mode, growth process is started with an initial two dimensional layer deposition on the substrate material. After a critical layer deposition thickness is achieved, the surface transforms into three dimensional highly strained dot structures that grow coherently on the surface [27].

When the thickness reached over a critical value, two or more dots generally merged into one larger dot and the strain energy is relaxed as dislocations were incorporated in the dots [28].

Figure 2.2 shows the result of further AFM analyses i.e. the density, average height and average diameter of the dots. The density of samples (a), (b), (c), and (d) were  $1.13 \times 10^{10} \text{ cm}^{-2}$ ,  $0.59 \times 10^{10} \text{ cm}^{-2}$ ,  $4.68 \times 10^{10} \text{ cm}^{-2}$ , and  $0.79 \times 10^{10} \text{ cm}^{-2}$ , respectively. AFM images also show the affect of buffer layer thickness on the density, height and diameter of the In<sub>0.5</sub>Ga<sub>0.5</sub>As nanostructures. When the buffer layer thickness is increased from 100 nm to 150 nm, the density of nanostructures is dramatically decreases from  $1.13 \times 10^{10} \text{ cm}^{-2}$  to  $0.59 \times 10^{10} \text{ cm}^{-2}$  and the dots become bigger with increase in diameter and height. On the other hand, the size of small dots decreases in diameter but increases in height with increasing buffer layer thickness. Sample (c) shows a sharp increase in the dot density and smaller average height and average diameter compared to other samples. The density of the dots reduced again dramatically for sample (d) where the buffer layer thickness was 300 nm. Sample (d) also has smaller dots compared with other samples, but it has several bigger dots similar to sample (b) in size. It was also clearly visible that the density of dots decreases as the number of larger dots (nano-island) increases on the surface.

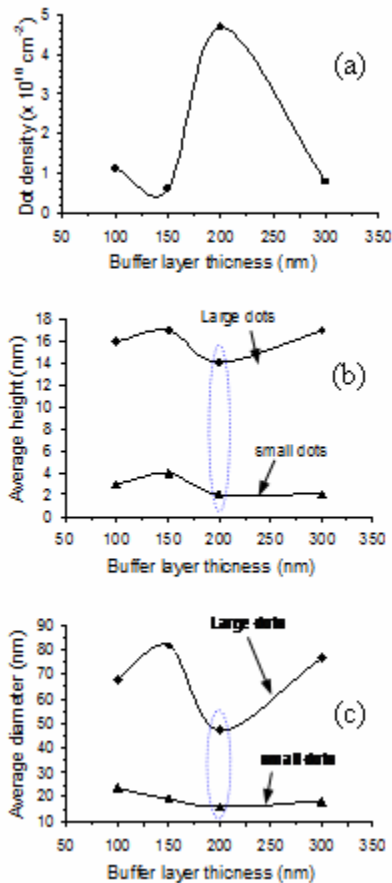


**Figure 2.2.** Area density, diameter and height of double  $\text{In}_{0.5}\text{Ga}_{0.5}\text{As}$  nanostructures as a function of GaAs buffer layer thickness.

The surface morphology of  $\text{In}_{0.5}\text{Ga}_{0.5}\text{As}$  nanostructures with different buffer layer thickness were also characterized by FESEM. Sample (a), (b), (c) and (d) show the  $\text{In}_{0.5}\text{Ga}_{0.5}\text{As}$  nanostructures grown with a 100 nm, 150 nm, 200 nm and 300 nm GaAs buffer layer thickness, respectively. All of these  $\text{In}_{0.5}\text{Ga}_{0.5}\text{As}$  nanostructures have different surface morphology of large and small dots distributed on the surface. Dots size variation ranging from 20-55 nm, 15-50 nm, 14-30 nm, and 12-60 nm for samples



(a), (b), (c), and (d), respectively. However, the small dots are not clearly visible as shown by the AFM.

It has been reported that surface morphology of In<sub>0.5</sub>Ga<sub>0.5</sub>As nanostructures is also influenced by the spacer layer thickness [29]. The first formation of the nanostructure will certainly affect the formation of the next dot. In another study by us showed that the single layer InGaAs nanostructures grown using different buffer layers have different surface morphology (result is not shown).

The other factor that affects the surface morphology is the inhomogeneous distribution of strains in the epilayer. This is the result of lattice mismatch between GaAs buffer layer and In<sub>0.5</sub>Ga<sub>0.5</sub>As which induces strain in the epilayer. At the beginning of In<sub>0.5</sub>Ga<sub>0.5</sub>As nanostructures growth, the strain energy will be accumulated both in the epilayer and at the top of GaAs buffer layer. Studies of InAs on GaAs(110) and GaAs(111) have indicated that epilayer grown on GaAs buffer layers of a few monolayers (MLs) in thickness can significantly affect the strain relaxation of the epilayer [19]. Different misfit strain produces stress fields at the surface, which is strong enough to affect the surface morphology evolution of the surface.

This study shows that GaAs buffer layer thickness has significant effect on the dot formation. The thickness of the 2D GaAs buffer layer before 3D nanostructure formation determines the statistics of the steps and terraces on the surface of GaAs buffer layer and thus influences the formation of the 3D structure. This is contradicting the result from the MBE growth which shows that the buffer roughness and step edge length do not determine the dots across the wafer [9]. In this case the formation of the nanostructure is dependent upon the kinetic process of the deposited adatom on the growing surface. Generally, the dynamic of the growth is introduced as a stochastic process for adsorption, evaporation, and surface migration. Adsorption and evaporation depend on the binding energy of adsorption to substrate i.e. on the sticking coefficient. The sticking coefficient is closely related to the critical the chemical reactivity of adsorbates with the substrate. The site and equilibrium structure of overlayers can be determined

by the chemical reactivity and surface of the adsorbates on the substrate. Anisotropy of surface diffusion coefficients can lead to a change in the shape of surface nanostructure, which is caused by the different capture moving in different directions.

## 2.4 CONCLUSION

Double layer  $\text{In}_{0.15}\text{Ga}_{0.85}\text{As}$  nanostructures have been grown on GaAs (100) substrate with various buffer layer thicknesses using MOVPE system. The surface morphology was investigated using AFM and FESEM. All samples  $\text{In}_{0.5}\text{Ga}_{0.5}\text{As}$  nanostructures have different size, density and uniformity and can be grouped into small and large dots. The size of small dots decreases with steadily increasing of the buffer layer thickness. Surface morphology was influenced by the inhomogeneous distribution of strain in the epilayer. The inhomogeneous distribution of strain in the rough buffer layer contributes this nanostructure morphology. Lattice strain and kinetic processes like surface diffusion and the incorporation of adatoms also contributed on the island formation. In this paper, the nanostructures formation depends of the statistics of the steps and terrace on the surface of GaAs buffer layer. Surface morphology and distribution of  $\text{In}_{0.5}\text{Ga}_{0.5}\text{As}$  nanostructures is dependent upon the growth parameter.

## 2.5 REFERENCES

- [1] H. Totsuka, E. Kurzt, T. Hanada, Z. Zhu, and T. Yao (1998). *J. Applied Surface Science* 130-132: 742-746.
- [2] D. Grützmacher, C. Dais, L. Zhang, E. Müller, H. H. Solak. *J. Materials Science and Engineering C* 27. (2007) 947–953.
- [3] Y. H. Jiao, J. Wu, B. Xu, P. Jin, L. J. Hu, L. Y. Liang, and Z. G. Wang. *J. Physica E* 35. (2006) 194-198.

- [4] J. S. Kim. *J. Korean Physical Society* 49. (2006) 195-198
- [5] K. Sears, J. Wong-Leung, H. H. Tan, C. Jagadish. *J. Crystal Growth* 281 (2005) 290–296
- [6] S. Anantathanasarn, Y. Barbarin, N.I. Cade, P.J. van Veldhoven, E.A.J.M. Bente, Y.S. Oei, H. Kamada, M.K. Smit, R. Notzel. *J. Materials Science and Engineering B* 147 (2008) 124–130
- [7] J. S. Kim, J. H. Lee, S. U. Hong, H. S. Kwack, C. W. Lee, and D. K. Oh. *ETRI Journal* 26 (5). (2004) 475-480
- [8] A. Roshko, T. E. Harvey, S. Y. Lehman, R. P. Mirin, K. A. Bertness and B. L. Hyland. *J. Vac. Sci. Technol. B* 23 (3), (2004) 1226-1231
- [9] C. M. Lai, F. Y. Chang, H. H. Lin and G. J. Jan. *J. Korean Physical Society* 42. (2003) S114-S119.
- [10] T. D. Germann, A. Strittmatter, Th. Kettler, K. Posilovic, U. W. Pohl, D. Bimberg. *J. Crystal Growth* 298. (2007) 591-594
- [11] D. Bimberg. *J. Appl. Phys.* 38. (2005) 2055-2058
- [12] K. Mukai, Y. Nakata, and M. Sugawara. *J Science Technology* 34. (1998) 223-234
- [13] T. P. Hsieh, H. S. Chang, W. Y. Chen, W. H. Chang, T. M. Hsu, N. T. Yeh, W. J. Ho. P. C. Chiu and J. I. Chyi. *J. Nanotechnology* 17. (2006) 512-515.
- [14] J. Temmyo, E. Kuramochi, M. Sugo, T. Nishiya, R. Notzel, and T. Tamamura. *J. Material Science and Engineering B* 35. (1995) 7-11.
- [15] F. Dimroth, P. Lanyi, U. Schubert, and A.W. Bett. *J. Electronic Materials* 29. (2000) 42-43
- [16] J. I. Chyi. *J. Material Science and engineering B* 75. (2000) 121-125.

- [17] L. Lazzarini, G. Salviati, S. Franchi and E. Napolitani. *J. Material Science and Engineering B* 80. (2001) 120-124
- [18] Z. C. Zhang, Y. H. Chen, S. Y. Yang, F. Q. Zhang, B. S. Ma, B. Xu, Y. P. Zeng, Z. G. Wang and X. P. Zhang. *J. Semiconductor Science Technology*. 18 (11). (2003) 955-959.
- [19] L. Daweritz, R. Hey, H. Berger. in: *Studies in Surface Science and Catalysis: Physics of Solid Surfaces*, Ed. J. Koukal, Elsevier Science Publisher, Netherlands, 1987, pp. 194-196
- [20] R. Leon, J. Wellman, X. Z. Liao, J. Zou, and D. J. H. Cockayne. *J. Applied Physics Letter* 76. (2000) 1558-1560
- [21] A. Roskho, T. E. Harvey, S. Y. Lehman, R. P. Mirin, K. A. Bertness and B. L. Hyland. *J. Vac. Sci. Technol. B* 23(3). (2005) 1226-1231
- [22] J. H. Lee, W. J. Choi, Y. J. Park, I. K. Han, J. I. Lee, W. J. Cho and E. K. Kim. *J. Phys Stat. Sol. (c)* 4. (2003) 1185-1188.
- [23] T. Mano, K. Watanabe, S. Tsukamoto, H. Fujioka, M. Oshima, N. Koguchi. *J. Crystal Growth* 209. (2000) 504-508
- [24] J. R. Ro, S. B. Kim, E. H. Lee and S. J. Park. *J. Microelectronic Engineering* 43-44. (1998) 11-18.
- [25] V. P. Kladko, V. V. Strelchuck, A. F. Kolomys, M. V. Slobodian, YU. I. Mazur, ZH.M. Wang, Vas. P. Kunets, and G. J. Salamo. *J. Electronic Materials* 36(12). (2007) 1555-1559.
- [26] M. Kawabe, in: *Physics, Chemistry and Application of Nanostructures*, Ed. V. E. Barisenko, S. V. Gaponenko and V. S. Gurin, World Scientific, Singapore, 2001. pp. 15-21
- [27] L. K. Yu, B. Xu, Z.G. Wang, P. Jin, C. Zhao, W. Lei, J. Sun, K. Li, L. J. Hu, and L.Y. Liang. *J. Crystal Growth* 282. (2005) 173-178.

- [28] J. He, Y. C. Zhang, B. Xu, and Z. G. Wang. *J. of Crystal Growth* 247. (2003) 49–54
- [29] H. Muller-Krumbhaar, in: *Monte Carlo Methods in Statistical Physics*, Ed. K. Binder, Springer, Berlin, 1979. pp. 261.